Ca^{2+} Modulation of Ca^{2+} Release-Activated Ca^{2+} Channels Is Responsible for the Inactivation of Its Monovalent Cation Current

Zhengchang Su,* Richard L. Shoemaker,* Richard B. Marchase,[†] and J. Edwin Blalock*

*Department of Physiology and Biophysics and [†]Department of Cell Biology, University of Alabama at Birmingham, Birmingham, Alabama 35294-0005

ABSTRACT   The Ca^{2+} release-activated Ca^{2+} (CRAC) channel is the most well documented of the store-operated ion channels that are widely expressed and are involved in many important biological processes. However, the regulation of the CRAC channel by intracellular or extracellular messengers as well as its molecular identity is largely unknown. Specifically, in the absence of extracellular divalent cations it becomes permeable to monovalent cations with a larger conductance, however this monovalent cation current inactivates rapidly by an unknown mechanism. Here we found that Ca^{2+} dissociation from a site on the extracellular side of the CRAC channel is responsible for the inactivation of its Na$^+$ current, and Ca^{2+} occupancy of this site otherwise potentiates its Ca^{2+} as well as Na$^+$ currents. This Ca^{2+}-dependent potentiation is required for the normal functioning of CRAC channels.

INTRODUCTION

Agonist-receptor interactions at the plasma membrane often lead to the generation of inositol 1,4,5-trisphosphate (IP$_3$) in many cell types, which in turn releases Ca^{2+} from internal stores in the endoplasmic reticulum. Such a depletion of Ca^{2+} stores somehow activates Ca^{2+} permeable store-operated ion channels (SOCs) in the plasma membrane, allowing a sustained Ca^{2+} influx termed capacitative or stored-operated Ca^{2+} entry (Putney and Bird, 1993). In lymphocytes, mast cells and rat basophilic leukemia (RBL) cells, depletion of internal Ca^{2+} stores by either antigen/agonist binding or sarcoplasmic/endoplasmic reticulum Ca^{2+} (SERCA) pump inhibitors (e.g., thapsigagin), or dialysis of the cytosol by a whole-cell pipette solution during patch-clamp recordings activate a highly Ca^{2+}-selective ion channel termed the Ca^{2+} release-activated Ca^{2+} (CRAC) channel (Lewis and Cahalan, 1989; Zweifach and Lewis, 1993; Hoth and Penner, 1992, 1993; Premack et al., 1994), which has an extremely low unitary conductance for Ca^{2+} (24 fs) (Zweifach and Lewis, 1993). Even though the CRAC channel is the most widely accepted, and well-characterized SOCs (Parekh and Penner, 1997), its molecular identity, activation mechanism, and regulation are yet to be fully determined.

One intriguing property of the CRAC channel is its high Ca^{2+} selectivity under normal physiological conditions. Its selectivity for Ca^{2+} is >1000 times higher than for Na$^+$, which is even higher than that of voltage-gated Ca^{2+} channels (Hoth and Penner, 1993). However, in the absence of any extracellular divalent cations, it becomes permeable to monovalent cations (Hoth and Penner, 1993; Premack et al., 1994) with a larger single-channel conductance (unitary

conductance = 2 pS for Na$^+$ (Prakriya and Lewis, 2002)). A similar phenomenon has been observed for voltage-gated Ca^{2+} channels (Almers et al., 1984; Fukushima and Hagiwara, 1985; Almers and McCleskey, 1984; Hess and Tsien, 1984; Hess et al., 1986). However, in contrast to voltage-gated Ca^{2+} channels where Na$^+$ and Ca^{2+} currents show similar kinetics (Almers et al., 1984; Fukushima and Hagiwara, 1985; Almers and McCleskey, 1984; Hess and Tsien, 1984; Hess et al., 1986), the Na$^+$ current through CRAC channels (Na$^+$-I$_{CRAC}$) inactivates rapidly by an unknown mechanism. The rapid inactivation of Na$^+$-I$_{CRAC}$ is interesting for two reasons: first, this type of inactivation has not been observed in any other well-known ion channels to our knowledge, and therefore might represent a new form of ion channel inactivation. Second, understanding the mechanism underling the inactivation of Na$^+$-I$_{CRAC}$ may reveal a novel regulatory mode for CRAC channels. In this study we have shown that the inactivation of Na$^+$-I$_{CRAC}$ is due to the dissociation of Ca^{2+} ions from a site on the outside of the CRAC channel, and Ca^{2+} binding to this site otherwise potentiates the current. Moreover, Ca^{2+} occupancy is necessary for the normal functioning of CRAC channels.

MATERIALS AND METHODS

Cell culture

Rat basophilic leukemia (RBL-2H3) cells were maintained as previously described (Su et al., 2002)

Patch clamp recordings

Whole-cell recordings were performed with RBL-2H3 cells at room temperature with an Axonpatch 200B amplifier (Axon Instruments, Fox City, CA). Standard external solution (SES) contained (in mM) 143 NaCl, 10 CaCl$_2$, 1 MgCl$_2$, 5 D-glucose, 4.5 KCl, 0.5 BaCl$_2$, and 10 HEPES, pH 7.3 adjusted with NaOH. Nominal Ca^{2+}-free solution was made by replacing Ca^{2+} in SES with equal-molar Mg^{2+}. The currents measured in this solution were used as leak currents for subtraction to eliminate possible contamination currents from Mg^{2+}-inhibited cation channels (Prakriya

and Lewis, 2002; Su et al., 2002). In some experiments as labeled in the figures (Figs. 3 *A* and 6 *C*), the external solution contained (in mM) 149 *N*-methyl-D-glutamine (NMDG) chloride, 10 $CaCl_2$ or $MgCl_2$ or $BaCl_2$ or $MnCl_2$ or $NiCl_2$ or $ZnCl_2$, 5 D-glucose, and 10 HEPES, pH 7.3 adjusted with NMDG. External solutions containing 50 or 1 mM Ca^{2+} used in Figs. 4 and 6 were made by replacing 10 mM Ca^{2+} in this solution with the corresponding molarity of Ca^{2+} and changing NMDG-Cl level to 89 or 162.5 mM to maintain the total osmolarity. External solutions containing from 10 nM to 100 μM free $[Ca^{2+}]$ used in Fig. 4 were made by adding an appropriate amount of $CaCl_2$ to the following metal-ions-free solution (MIF) containing (in mM) 158 NMDG-Cl, 10 HEPES, 5 glucose, and 2 NMDG-EGTA, pH 7.3 adjusted by NMDG. The divalent cation free solution (DVF) contained (in mM) 160 Na-methane sulphonate, 5 D-glucose, 2 Na-EGTA, and 10 HEPES, pH 7.2 adjusted with NaOH. External solutions containing from 10 nM to 100 μM free $[Ca^{2+}]$ used in Fig. 5 *A* were made by adding appropriate amounts of $CaCl_2$ to DVF. Standard internal solution for whole-cell recordings contained (in mM) 110 Cs-glutamate, 10 CsCl, 2.9 $MgCl_2$, 0.6 $CaCl_2$, 10 Cs-EGTA, and 30 HEPES, pH 7.2 adjusted with CsOH. The calculated free $[Ca^{2+}]$ and $[Mg^{2+}]$ are 10 nM and 2 mM, respectively. The whole-cell currents shown in Figs. 1 *A*, 3 *A*, 5 *A*, and 6 *C* were detected by applying a 100-ms voltage ramp from -100 to 100 mV at a frequency of 1 Hz while cells were held at -40 mV, and currents at -80 mV are displayed. The whole-cell currents shown in Fig. 7 were detected by applying an 80-ms voltage step of -80 mV at a frequency of 2 Hz while cells were held at $+60$, 0, or -60 mV. The signal was filtered at 1 kHz with a built-in lowpass Bessel filter of the amplifier and digitized at 5 kHz. In all other experiments to detect the fast transition of the currents, the currents were continuously measured at -60 mV, filtered at 1 kHz with the built-in lowpass Bessel filter of the amplifier, and digitized at 5 kHz. Fast solution exchange was achieved using a mobile linear array of wide-tipped puffer pipettes. Only experiments with a solution exchange time <150 ms were included in the analysis.

Data analysis

The activation and inactivation time courses of CRAC channels were fitted to the equations:

$$I = I_0 + I_1 \exp(-t/\tau) \quad or$$
$$I = I_0 + I_1 \exp(-t/\tau_1) + I_2 \exp(-t/\tau_2),$$

using pClampfit 8.0 (Axon Instruments), where I = current, t = time, I_0, I_1, and I_2 are constants, τ, τ_1, and τ_2 are the activation or inactivation time constants. The dose-response data shown in Figs. 4 *E* and 5 *D* were fitted to the Hill equation:

$$i = i_{max}/(1 + (K_d/[Ca^{2+}]^n)) + i_0,$$

where i is the inactivation index of Na^+-I_{CRAC} (for definition, see below); i_{max} and i_0 are constants; K_d, the dissociation constant; $[Ca^{2+}]$, Ca^{2+} concentration; and n, the Hill coefficient. Data in Fig. 5 *B* were also fitted to a similar Hill equation. Data were shown as mean $\pm$SD if appropriate, and the two-tail *t*-test was used for statistical analyses.

RESULTS

Inactivation of the Na^+ current through CRAC channels

As shown in Fig. 1 *A*, after whole-cell break-in on an RBL cell, dialysis of the cytosol of the cell with pipette solution spontaneously activated Ca^{2+}-I_{CRAC} (Ca^{2+} current through CRAC channels) and Na^+-I_{CRAC} in parallel while the external solution was alternated between SES and DVF as indicated by the labeled horizontal bars. The identities of
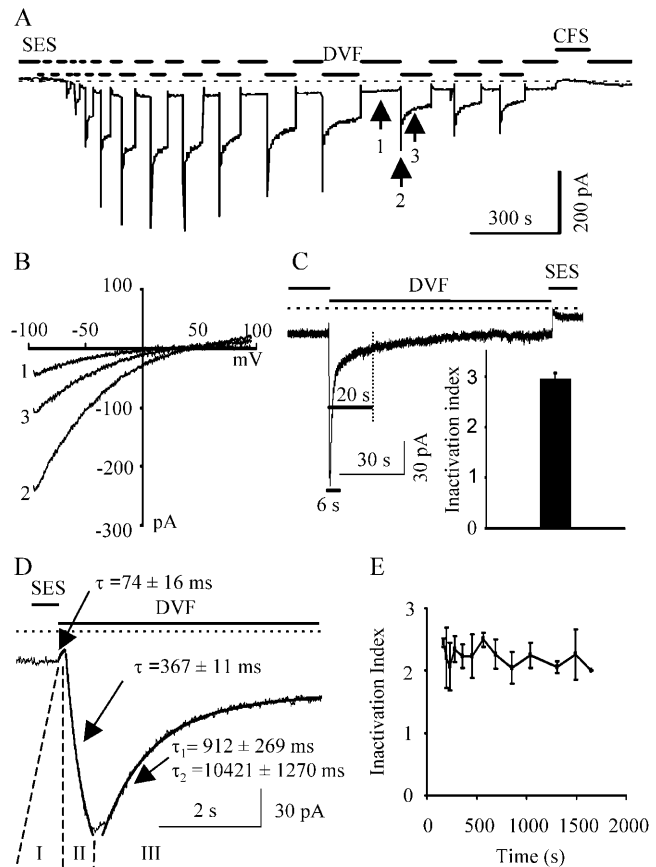

FIGURE 1 Inactivation of Na^+-I_{CRAC}. (*A*) Whole-cell break-in on an RBL-2H3 cell activated Ca^{2+}-I_{CRAC} and Na^+-I_{CRAC} when the external solution was alternated between standard extracellular solution (containing (in mM) 143 NaCl, 10 $CaCl_2$, 1 $MgCl_2$, 5 D-glucose, 4.5 KCl, 0.5 $BaCl_2$, and 10 HEPES) and divalent-free solution (containing (in mM) 160 Na-methane sulphonate, 5 D-glucose, 2 Na-EGTA, and 10 HEPES). The current was detected by applying voltage ramps at 1 Hz and the values at -80 are displayed. Note that Ca^{2+}-free solution (containing (in mM) 143 NaCl, 11 $MaCl_2$, 5 D-glucose, 4.5 KCl, 0.5 $BaCl_2$, and 10 HEPES) completely abolished the I_{CRAC}. The horizontal dotted lines represent 0 current level in this and the following figures. (*B*) The I-V relationships of the current taken at the corresponding number-labeled time points in panel *A* when it reached steady state of Ca^{2+}-I_{CRAC} (trace 1), peak of Na^+-I_{CRAC} (trace 2), and steady state of Na^+-I_{CRAC} (trace 3). (*C*) The current from another cell was continuously recorded under -60 mV to reveal the fast kinetics of the transient current during the solution exchange. (*inset*) The inactivation index (see text for definition) of the Na^+-I_{CRAC} when the extracellular solution was exchanged from SES to DVF, $n = 16$. (*D*) The segment of the current (6-s long) as indicated by the horizontal bar near the peak of the current in panel *C* is displayed on an expanded timescale, revealing a three-phase kinetics of the current during the solution exchange. The smooth lines are the fitting curves for the preactivation (I), activation (II), and inactivation (III) phases of the Na^+-I_{CRAC}, $n = 16$. (*E*) Inactivation index of Na^+-I_{CRAC} as a function of time after whole-cell break-in. Data are pooled from experiments as in panel *A*, $n = 4$.

Ca^{2+}-I_{CRAC} and Na^+-I_{CRAC} were evidenced by their inwardly rectifying I-V relationships and positive reversal potentials (>50 mV for Ca^{2+}-I_{CRAC} and 50 mV for Na^+-I_{CRAC}) (Fig. 1 *B*) (Su et al., 2002). Notably, although Na^+-I_{CRAC} was initially larger, it inactivated rapidly (Fig. 1 *A*).

A similar phenomenon was seen when Na$^+$ was replaced by Li$^+$ or K$^+$ (data not shown). This confirms the previous similar observations in Jurkat T (Prakriya and Lewis, 2002), rat mast (Hoth and Penner, 1992, 1993), and RBL cells (Kozak et al., 2002; Hermosura et al., 2002). To reveal the details of the transition of the current during the solution exchange, we continuously recorded the current from other cells with a higher signal-sampling rate under a holding potential of −60 mV (see Materials and Methods). As shown in Fig. 1, C and D, such recordings revealed that the kinetics of the current induced by solution exchange consists of three phases (Fig. 1 D). In phase I, the current first slightly decreased when the Ca^{2+}-containing solution SES was changed to DVF (Fig. 1 D). This phase can be fitted to a single-component exponential equation with a time constant of 74.0 ± 16.3 ms ($n = 20$), which reflects the rate of solution exchange to remove the Ca^{2+} blockage of Na$^+$-I$_{CRAC}$ (Fig. 1 D). We therefore termed this phase the preactivation phase of Na$^+$-I$_{CRAC}$. In phase II, the current rapidly increased to a maximum (peak) in 779.1 ± 87.2 ms ($n = 17$), reflecting the activation process of Na$^+$-I$_{CRAC}$, and we thus termed it the activation phase of Na$^+$-I$_{CRAC}$. It can be fitted to a single-component exponential equation with a time constant of 367.2 ± 11.0 ms ($n = 17$) (Fig. 1 D). The current then rapidly inactivated to a steady state in phase III, so we termed this phase the inactivation phase of Na$^+$-I$_{CRAC}$. It can be fitted to a two-component exponential equation with time constants $\tau_1 = 912.0 \pm 269.0$ ms and $\tau_2 = 10421.4 \pm 1270.0$ ms ($n = 17$) (Fig. 1 D). To quantitatively analyze the inactivation of the Na$^+$-I$_{CRAC}$, we defined an inactivation index as the ratio of the peak Na$^+$-I$_{CRAC}$ and the Na$^+$-I$_{CRAC}$ measured at 20 s after the peak (Fig. 1 C):

$$\text{Inactivation index} = I_{peak}/I_{20\,s\,after\,peak}.$$

The 20-s measurement was chosen to reflect the fact that the Na$^+$-I$_{CRAC}$ inactivates to a steady state in 20 s after reaching the peak (Fig. 1 C). The inactivation index of Na$^+$-I$_{CRAC}$ is 2.9 ± 0.14 ($n = 16$) when the extracellular solution was switched from SES to DVF (Fig. 1 C inset). As shown in Fig. 1 E, the inactivation index remained relatively stable during the activation and slow inactivation of CRAC channels (Zweifach and Lewis, 1995b; Parekh, 1998), suggesting that it is a useful parameter with which to investigate effects of the other factors on the rapid inactivation of Na$^+$-I$_{CRAC}$.

Preexposing cells to metal ions confers the three-phase kinetics of I$_{CRAC}$ during the solution exchange

Because the complex three-phase kinetics of the I$_{CRAC}$ occurred when all the metal ions were replaced by Na$^+$, we tested the effects of preexposure of cells to cations on the kinetics of Na$^+$-I$_{CRAC}$. As shown in Fig. 2 A, preexposing a cell to the MIF solution (see Materials and Methods) before
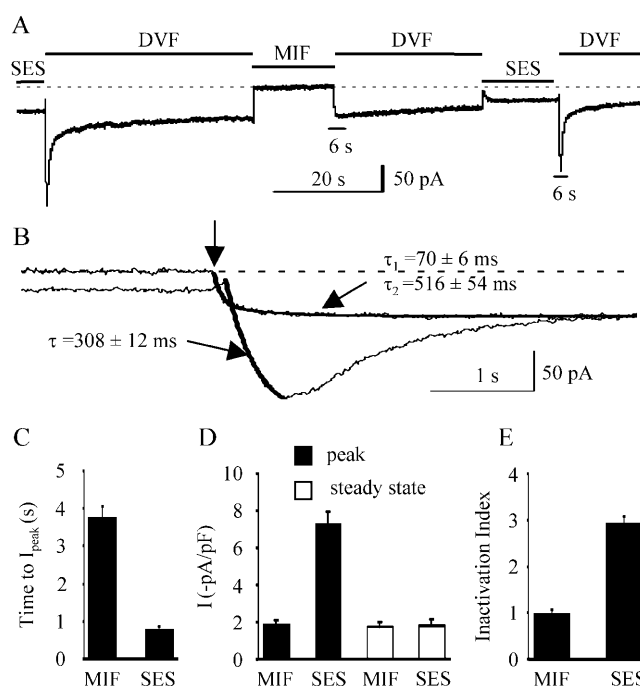

FIGURE 2 Preexposing cells to metal ions confers the three-phase kinetics of the I$_{CRAC}$ during solution exchange. (A) Preexposing a cell to metal-ions-free solution (containing (in mM) 158 NMDG-Cl, 10 HEPES, 5 glucose, and 2 NMDG-EGTA) completely abolished the three-phase kinetics of I$_{CRAC}$, and greatly reduced the peak value of the Na$^+$-I$_{CRAC}$. Reexposing the cell to SES restored the three-phase kinetics of the current and the peak value of Na$^+$-I$_{CRAC}$. (B) The two segments of current (6-s long) as indicated by the horizontal bars labeled ''6 s'' in panel A are displayed on an expanded timescale to show the detailed kinetics of the current during the solution exchanges. The smooth lines are the fitting curves for the activation phases when the cells were preexposed to SES ($n = 18$) or to MIF ($n = 7$). The vertical arrow indicates the initiation of the solution exchange. (C) The time to peak for Na$^+$-I$_{CRAC}$ when the cells were preexposed to MIF ($n = 7$) or to SES ($n = 18$). (D) The normalized peak or steady-state Na$^+$-I$_{CRAC}$ when the cells were preexposed to MIF ($n = 7$) or to SES ($n = 18$). (E) The inactivation indices of Na$^+$-I$_{CRAC}$ when cells were preexposed to MIF ($n = 7$) or to SES ($n = 18$).

switching to DVF abolished the three-phase kinetics of I$_{CRAC}$ during solution exchange and greatly reduced the size of peak Na$^+$-I$_{CRAC}$. However, preexposing the cell to the SES before switching to DVF restored the three-phase kinetics of the I$_{CRAC}$ (Fig. 2 A) and to a large extent the size of the peak Na$^+$-I$_{CRAC}$. The smaller size of the restored peak Na$^+$-I$_{CRAC}$ is due to the unavoidable slow inactivation of the CRAC channel (Zweifach and Lewis, 1995b; Parekh, 1998). As shown in Fig. 2 B, superimposing the two segments (6-s long) of current as indicated by the horizontal bars labeled ''6 s'' in Fig. 2 A over time revealed some marked contrasts in kinetics of the currents. First, when the cells were preexposed to MIF, the Na$^+$-I$_{CRAC}$ activated almost immediately after switching to DVF, whereas when the cells were preexposed to SES, the current first underwent the preactivation phase of the Na$^+$-I$_{CRAC}$, i.e., the current first decreased before the Na$^+$-I$_{CRAC}$ developed (Fig. 2 B).

Second, when the cells were preexposed to MIF, the time for Na^{+}-I_{CRAC} to develop to its peak (time to peak) was longer (3.73 ± 0.34 s, $n = 7$) compared to that when the cells were preexposed to SES (0.78 ± 0.09 s, $n = 18$) (Fig. 2, B and C). The activation time course, when the cells were preexposed to MIF, can be fitted to a two-component exponential equation with time constants $\tau_1 = 70.1 \pm 5.5$ ms and $\tau_2 = 516.1 \pm 53.8$ ms ($n = 7$) (Fig. 2 B), whereas that when the cells were exposed to SES can be fitted to a single-component exponential equation with a time constant of 308.2 ± 12.0 ($n = 18$). (Fig. 2 B). Third, the magnitude of the peak Na^{+}-I_{CRAC} when the cells were preexposed to MIF is only about the same size as the steady-state Na^{+}-I_{CRAC} when the cells were preexposed to SES (Fig. 2, A and D). Fourth, the inactivation index of Na^{+}-I_{CRAC} when cells were preexposed to MIF is close to 1 (0.99 ± 0.08, $n = 7$) (Fig. 2 E), indicating that there is no further inactivation of Na^{+}-I_{CRAC} after preexposing to MIF. These results strongly suggest that preexposure of the cell to MIF has already inactivated the current to a steady state, and therefore it cannot be further inactivated. In other words, preexposure of cells to the SES potentiates Na^{+}-I_{CRAC}, whereas preexposure of cells to MIF inactivates it. We therefore hypothesized that association of a metal ion to a site on the CRAC channel might potentiate Na^{+}-I_{CRAC}, whereas its dissociation from this site might result in the inactivation of the Na^{+}-I_{CRAC}.

Ca^{2+} dissociation from a binding site on the CRAC channel is responsible for the inactivation of Na^{+}-I_{CRAC}

Because Ca^{2+}, as well as the CRAC channel blocker Ni^{2+} has been reported to potentiate the Ca^{2+}-I_{CRAC} in Jurkat T cell (Zweifach and Lewis, 1996; Christian et al., 1996), we tested the effect of various divalent cations on the inactivation of the Na^{+}-I_{CRAC}. As shown in Fig. 3 A, preexposing a cell to 10 mM Ca^{2+} (Ca^{2+} is the only metal cation in the solution; see Materials and Methods) greatly potentiated Na^{+}-I_{CRAC} that inactivated rapidly. Both its peak value (-7.85 ± 0.73 pA/pF, $n = 7$; Fig. 3 B) and inactivation index (2.84 ± 0.15, $n = 7$; Fig. 3 C) are similar to those seen when the cells were preexposed to SES (Fig. 2, D and E). However, preexposing the cell to the CRAC channel blockers Ni^{2+} or Zn^{2+} at 10 mM, failed to potentiate Na^{+}-I_{CRAC} as evidenced by a small peak Na^{+}-I_{CRAC} (-1.55 ± 0.12 pA/pF, $n = 6$ for Ni^{2+} and -1.6 ± 0.14 pA/pF, $n = 6$ for Zn^{2+}) and an inactivation index of ~ 1 (-1.01 ± 0.01, $n = 6$ for Ni^{2+} and 1.02 ± 0.03, $n = 6$ for Zn^{2+}). Preexposing the cell to 10 mM Ba^{2+}, Mn^{2+}, or Mg^{2+} only slightly potentiated Na^{+}-I_{CRAC}, because the current had a smaller peak Na^{+}-I_{CRAC} (-2.57 ± 0.44 pA/pF, $n = 7$, for Ba^{2+}; -2.63 ± 0.55 pA/pF, $n = 6$ for Mn^{2+}; and -2.50 ± 0.57 pA/pF, $n = 7$ for Mg^{2+}; Fig. 3 B) and a smaller inactivation index (1.34 ± 0.11, $n = 7$ for Ba^{2+}; 1.32 ± 0.09, $n = 6$ for Mn^{2+}; and 1.25 ± 0.09, $n = 7$ for Mg^{2+}; Fig. 3 C). Reexposing the cell to 10 mM Ca^{2+}
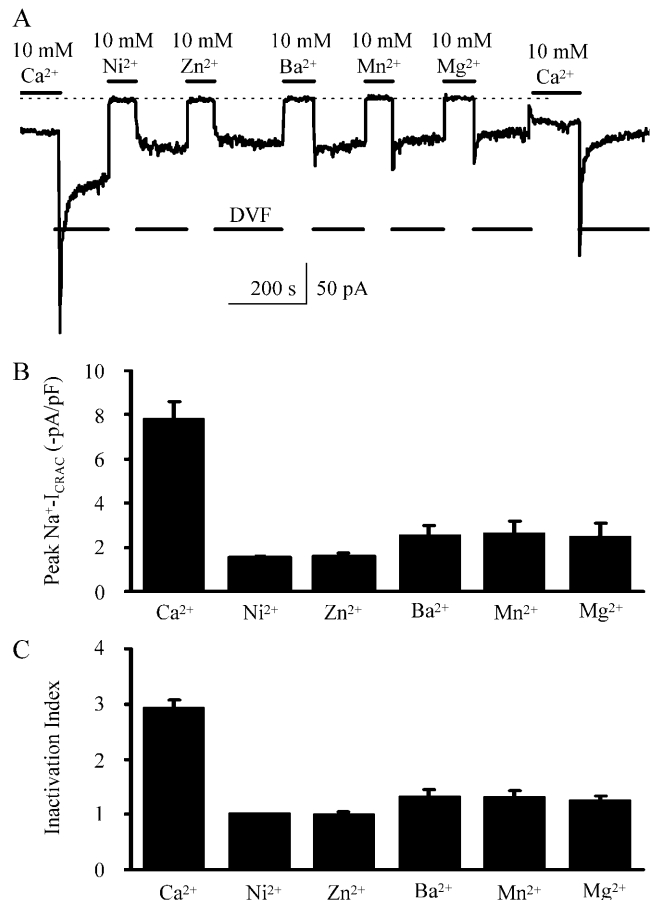

FIGURE 3 Ca^{2+} dissociation from a site on the CRAC channel is responsible for the inactivation of Na^{+}-I_{CRAC}. (A) Preexposing a cell to 10 mM Ca^{2+} (the solution contained (in mM) 149 N-methyl-D-glutamine chloride, 10 $CaCl_2$, 5 D-glucose, and 10 HEPES) greatly potentiated Na^{+}-I_{CRAC} that inactivated rapidly. Preexposing the cell to 10 mM Ni^{2+} or Zn^{2+} (replacing $CaCl_2$ by equal-molar $NiCl_2$ or $ZnCl_2$ in the above solution) failed to potentiate the Na^{+}-I_{CRAC}. Preexposing the cell to 10 mM Ba^{2+} or Mn^{2+} or Mg^{2+} (replacing $CaCl_2$ by equal-molar $BaCl_2$, $MnCl_2$, or $MgCl_2$ in the above solution) only partially potentiated the Na^{+}-I_{CRAC}. Reexposing the cell to 10 mM Ca^{2+} restored the potentiation. (B) The peak Na^{+}-I_{CRAC} when cells were preexposed to 10 mM Ca^{2+} ($n = 7$), Ni^{2+} ($n = 6$), Zn^{2+} ($n = 6$), Ba^{2+} ($n = 7$), Mn^{2+} ($n = 6$), or Mg^{2+} ($n = 7$). (C) The inactivation indices of Na^{+}-I_{CRAC} when cells were preexposed to 10 mM Ca^{2+} ($n = 7$), Ni^{2+} ($n = 6$), Zn^{2+} ($n = 6$), Ba^{2+} ($n = 7$), Mn^{2+} ($n = 6$), or Mg^{2+} ($n = 7$).

restored the potentiation and inactivation index of the Na^{+}-I_{CRAC} (Fig. 3 A). These results strongly suggest that Ca^{2+} is the most potent cation for potentiating Na^{+}-I_{CRAC}. Surprisingly, though Ca^{2+}-I_{CRAC} in Jurkat T cells is potentiated by Ni^{2+} (Zweifach and Lewis, 1996; Christian et al., 1996), Na^{2+}-I_{CRAC} in RBL-2H3 cells is not by either Ni^{2+} or Zn^{2+}.

By preexposing cells to solutions containing various levels of free Ca^{2+} with NMDG as the only other cation (see Materials and Methods) followed by exposure to DVF, we further showed that extracellular Ca^{2+} can dose-dependently potentiate Na^{+}-I_{CRAC} (Fig. 4, A and B). To eliminate the effects of the slow inactivation of I_{CRAC}, we cycled through the preexposing Ca^{2+} levels in both increasing and de-
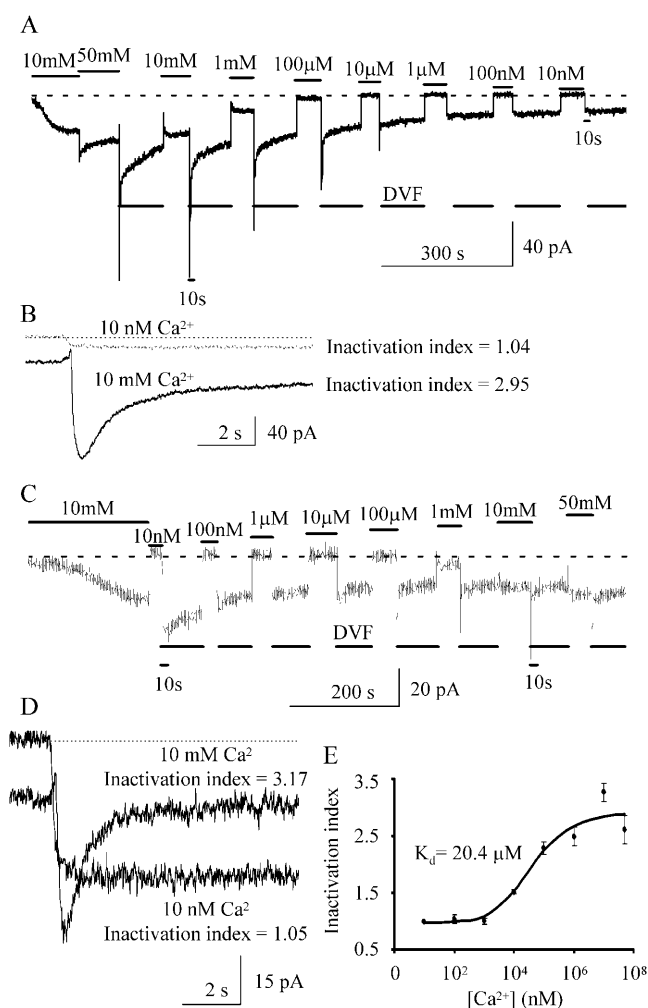
FIGURE 4 Extracellular Ca^{2+} ions dose-dependently potentiate Na$^+$-I$_{CRAC}$. Preexposing solutions containing 10 nM $\sim$100 μM Ca^{2+} levels were made by adding an appropriate amount of CaCl$_2$ to MIF containing (in mM) 158 NMDG-Cl, 10 HEPES, 5 glucose, and 2 NMDG-EGTA. Preexposing solutions containing 1, 10, or 50 mM Ca^{2+} were made by adding the required CaCl$_2$ to solutions containing (in mM) 162.5, 149, or 89 N-methyl-D-glutamine chloride, respectively, as well as 5 D-glucose and 10 HEPES. (A) After I$_{CRAC}$ was fully activated, the cell was preexposed to decreasing levels of Ca^{2+}, and each was followed by exposure to DFV. (B) The two segments of current (10-s long) as indicated by the horizontal bars labeled "10 s" in panel A are superimposed and displayed on an expanded timescale to show the detailed kinetics of the current during the solution exchanges when the cell was preexposed to 10 mM and 10 nM Ca^{2+}, with an inactivation index of 2.95 and 1.04, respectively. (C) After I$_{CRAC}$ was fully activated, the cell was preexposed to increasing levels of Ca^{2+}, and each was followed by exposing to DFV. (D) The two segments of current (10-s long) as indicated by the horizontal bars labeled "10 s" in panel C are superimposed and displayed on an expanded time scale to show the detailed kinetics of the current during the solution exchanges when the cell was preexposed to 10 mM and 10 nM Ca^{2+}, with an inactivation index of 3.17 and 1.05, respectively. (E) The dose-response relationship of the inactivation index and preexposing Ca^{2+} level. Data are pooled from eight experiments as shown in panels A and C, the smooth curve is a fitting to a Hill equation, yielding a $K_d = 20.4$ μM.

creasing orders. Similar results were obtained in both sets of experiments (Fig. 4, C and D). Fig. 4, B and D are examples of two superimposed 10-s segments of current taken from Fig. 4, A and C, as indicated by the horizontal bars labeled as "10 s" in Fig. 4, A and C, respectively. The inactivation indices for the same preexposing Ca^{2+} levels (1 nM and 10 mM) are similar, no matter whether preexposing Ca^{2+} levels were applied increasingly or decreasingly, suggesting that this ordering has little effect on the inactivation of Na$^+$-I$_{CRAC}$, even though the current undergoes unavoidable slow inactivation. This again suggests that an inactivation index is a good measure of Na$^+$-I$_{CRAC}$ inactivation. Fig. 4 E shows the pooled data from both types of experiments. Fitting the data to a Hill equation yielded a K_d of 20.4 μM. However, this value of K_d is likely to be an overestimate of the real value for the Ca^{2+} binding site, because the preexposing Ca^{2+} levels are used in the calculation. This concentration is rapidly diluted by DVF, and hence the actual Ca^{2+} levels around the channel are likely to be lower than the preexposing levels (a more accurate estimation of the K_d is given below). Nevertheless, these results strongly suggested that Ca^{2+} binding to a specific site on the CRAC channel potentiates Na$^+$-I$_{CRAC}$ and that dissociation of Ca^{2+} from it inactivates Na$^+$-I$_{CRAC}$. We thus termed this site a Ca^{2+}-dependent potentiation site (or a potentiation site for simplicity). A Ca^{2+}-binding site on the extracellular side of the CRAC channel has been suggested to account for the potentiation of the Ca^{2+} current in Jurkat T cells (Zweifach and Lewis, 1996; Christian et al., 1996).

The affinity of the potentiation site for Ca^{2+} is higher than that of the permeation site

The sequential rapid activation and inactivation of the Na$^+$-I$_{CRAC}$ might reflect a relief of Ca^{2+} blockage of Na$^+$-I$_{CRAC}$ and subsequent dissociation of Ca^{2+} from the potentiation site when the extracellular solution was rapidly switched from a Ca^{2+}-containing one to DVF. In other words, Ca^{2+} ions may be removed from the site in the channel that would otherwise prevent Na$^+$ from entering the pore before they dissociate from the potentiation site. We term this site a permeation site, and presume that it is located in the selectivity filter, as has been suggested for the voltage-gated Ca^{2+} channels (Ellinor et al., 1995b; Yang et al., 1993b). To test this, we preexposed cells to SES followed by exposure to solutions containing various levels of free Ca^{2+}, with Na$^+$ as the only other cation (see Material and Methods). As shown in Fig. 5 A, higher levels (>1 μM) of Ca^{2+} inhibited Na^{2+}-I$_{CRAC}$. Similar results were obtained when the Ca^{2+} levels were applied in a reverse order (data not shown). Fig. 5 B shows the pooled relationship of the steady-state Na$^+$-I$_{CRAC}$ (measured 20 s after peak; see Fig. 1 C) and the perfusing Ca^{2+} levels ($\geq$1 μM) from both types of experiments. Fitting the data to a Hill equation yielded a K_d of 13.7 μM (Fig. 5 B, $n = 5$). This K_d reflects the affinity of the
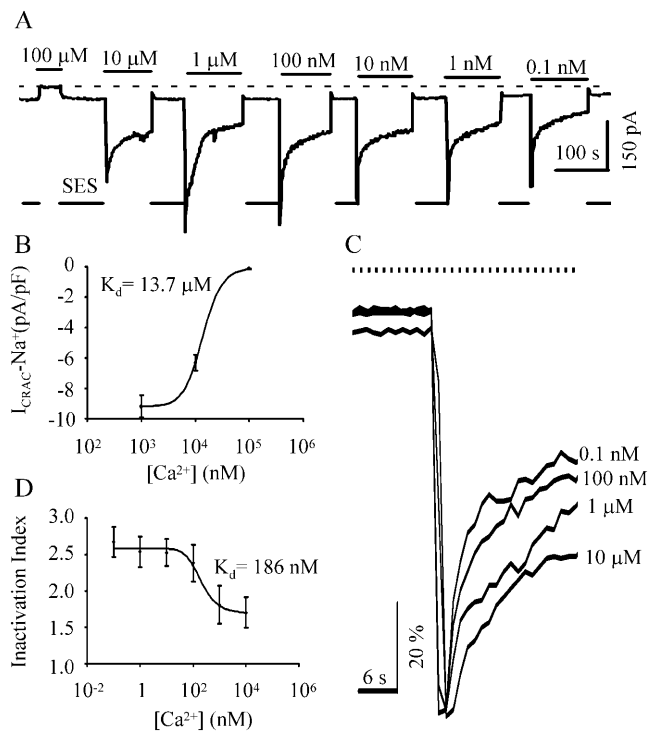
FIGURE 5 Ca^{2+} dissociates from the permeation site before it dissociates from the potentiation site. (*A*) A representative experiment to show that extracellular Ca^{2+} dose-dependently potentiates and blocks Na^+-I_{CRAC}. Cells were first exposed to SES followed by exposure to solutions containing various levels of free Ca^{2+} made by adding appropriate amount of $CaCl_2$ to the DVF containing (in mM) 160 Na-methane sulphonate, 5 D-glucose, 2 Na-EGTA, and 10 HEPES. (*B*) The steady-state Na^+-I_{CRAC} (measured at 20 s after peak) as a function of $[Ca^{2+}]$ in the perfusion solutions ($n = 5$). Fitting the data to a Hill equation yielded a K_d of 13.7 μM. (*C*) Extracellular Ca^{2+} dose-dependently delays the inactivation of Na^+-I_{CRAC}. Traces taken from panel *A* were normalized to their respective peak Na^+-I_{CRAC} and aligned at the time of the initiation of solution exchange. (*D*) The inactivation index of Na^+-I_{CRAC} as a function of $[Ca^{2+}]$ in the perfusion solutions ($n = 5$). Fitting the data to a Hill equation yielded a K_d of 186 nM.

permeation site for Ca^{2+} to block Na^+-I_{CRAC}. Interestingly, superimposing the activation and inactivation processes of normalized Na^+-I_{CRAC} recorded in various levels of free Ca^{2+} (≤ 10 μM) reveals that Ca^{2+} dose-dependently delayed the inactivation of Na^+-I_{CRAC} (Fig. 5 *C*), which is consistent with the idea that dissociation of Ca^{2+} from the potentiation site inactivates the Na^+-I_{CRAC}. Fig. 5 *D* is a plot of the pooled inactivation index of Na^+-I_{CRAC} as a function of $[Ca^{2+}]$ of the perfusion solutions. Fitting these data to a Hill equation yielded a K_d of 186 nM (Fig. 5 *D*, $n = 5$). This K_d seems to be a more accurate estimate of the dissociation constant of the potentiation site, because when Na^+-I_{CRAC} reaches the peak value used to compute the inactivation index (Fig.1 *C*), the preexposing solution has been fully washed out. Thus, it has little effect on the Ca^{2+} levels in the subsequent perfusion solutions. Therefore, the Ca^{2+} levels in this calculation are now likely to reflect the actual Ca^{2+} levels around the channel. Hence, this K_d reflects the affinity

of the potentiation site for Ca^{2+}, which is lower than the K_d for the Ca^{2+} permeation site. These results demonstrate that the affinity of the potentiation site for Ca^{2+} is higher than that of the permeation site, and therefore, a level of $[Ca^{2+}]$ can be reached such that the potentiation site is occupied by Ca^{2+} ions whereas the permeation site is not. Taken together, these results strongly suggest that Ca^{2+} ions are removed from the permeation site before they dissociate from the potentiation site during solution exchange.

Ca^{2+} occupancy of the potentiation site is required for the normal functioning of CRAC channels

In RBL-2H3 cells, Parekh and Penner (1997) have reported that they failed to see a similar potentiation of I_{CRAC} by Ca^{2+} as reported for the Jurkat T cells (Zweifach and Lewis, 1996; Christian et al., 1996). As a result of our finding with Na^+-I_{CRAC}, we revisited the effect of the Ca^{2+} binding on potentiation of the Ca^{2+}-I_{CRAC} channels in RBL-2H3 cells. As shown in Fig. 6, *A* and *B*, when a cell was preexposed to 10 mM Ca^{2+}, and thus the potentiation sites were presumably fully occupied by Ca^{2+}, increasing the extracellular Ca^{2+} level to 50 mM rapidly increased the I_{CRAC} due to a larger driving force. The time course of the current increase can be fitted to a single-component exponential equation with a time constant of 49.1 $\pm$ 12.5 ms ($n = 8$) (Fig. 6 *B*). In contrast, after occupying Ca^{2+} ions were fully washed away by DVF, an increase in the extracellular Ca^{2+} level to 50 mM first inhibited Na^+-I_{CRAC} and later only slowly increased the Ca^{2+} current (Fig. 6, *A* and *B*). The time course of this Ca^{2+}-I_{CRAC} increase phase could also be fitted to a single-component exponential equation but with a much longer time constant of 509.6 $\pm$ 60.9 ms ($n = 6$) (Fig. 6 *B*). These results strongly suggest that Ca^{2+} binding to the potentiation site also potentiates the Ca^{2+}-I_{CRAC}. The reason that Parekh and Penner (1997) failed to see the Ca^{2+} dependent potentiation of Ca^{2+}-I_{CRAC} is probably due to a different protocol. For example, if the rate of solution exchange is slow, such potentiation is masked (Z. Su and J. E. Blalock, unpublished observation). However, in contrast to the previous finding (Zweifach and Lewis, 1996; Christian et al., 1996) in Jurkat T cells, the CRAC channel blockers Ni^{2+} and Zn^{2+} failed to potentiate Ca^{2+}-I_{CRAC} in RBL-2H3 cells. The time course of Ca^{2+}-I_{CRAC} increase after the cells were preexposed to 10 mM Zn^{2+} or Ni^{2+} could be fitted to a two-component exponential equation with time constants $\tau_1 = 15.5 \pm 2.9$ s, $\tau_2 = 91.8 \pm 11.5$ s, $n = 6$ for Zn^{2+}, and $\tau_1 = 3.6 \pm 0.6$ s and $\tau_2 = 69.5 \pm 3.4$ s, $n = 6$ for Ni^{2+} (Fig. 6, *C* and *E*). These are significantly slower than the time constant when cells were preexposed to 10 mM Ca^{2+} ($\tau = 49.1 \pm 12.5$ ms; Fig. 6 *B*, $P < 0.001$). Ba^{2+}, Mn^{2+}, and Mg^{2+} may partially potentiate Ca^{2+}-I_{CRAC}, because the time course of the current increase after the cell was preexposed to these ions could be fitted to a single-component exponential equation with a time
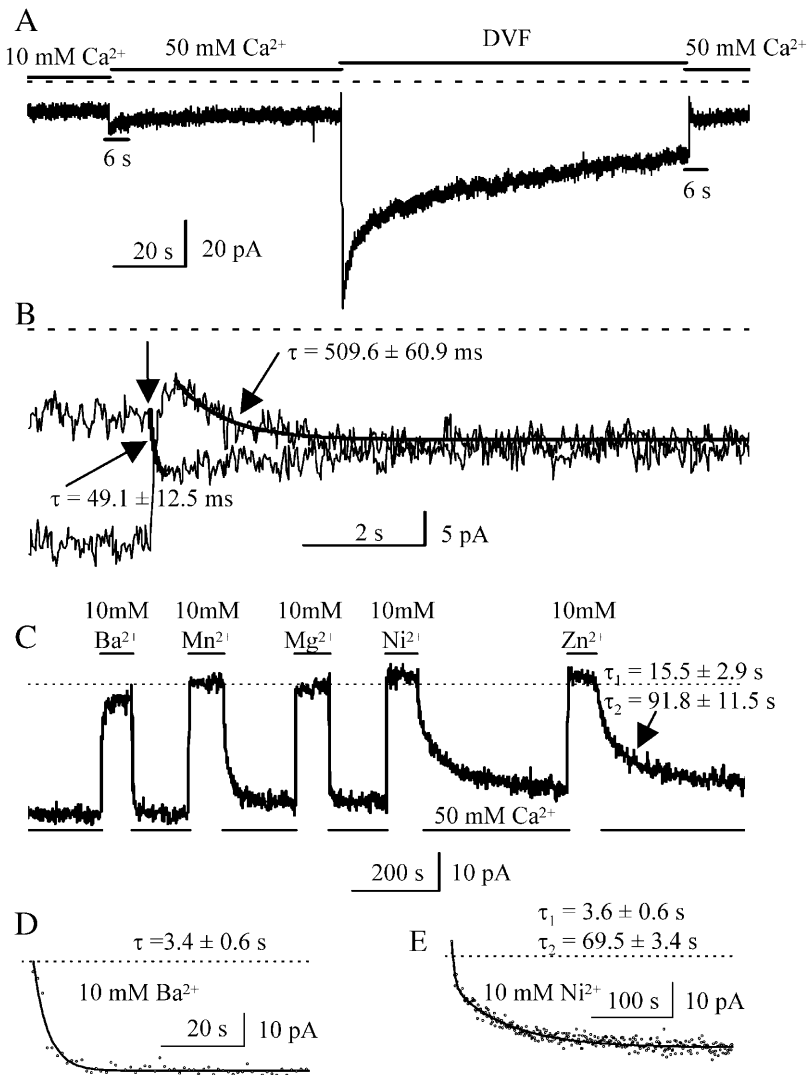
FIGURE 6 Ca^{2+} binding to the potentiation site is required for the functioning of CRAC channels. (A) I$_{CRAC}$ of a cell preexposed to 10 mM Ca^{2+} increased rapidly when the extracellular Ca^{2+} concentration was increased to 50 mM. However, when the cell was preexposed to DVF, subsequent exposing the cell to 50 mM Ca^{2+} rapidly inhibited Na^{+}-I$_{CRAC}$, which was then followed by a slow increase in Ca^{2+}-I$_{CRAC}$. Solutions containing 10 or 50 mM Ca^{2+} were made by adding the required CaCl$_2$ to a solution containing (in mM): 149 or 89 N-methyl-D-glutamine (NMDG) chloride, respectively, as well as 5 D-glucose, and 10 HEPES. (B) The two segments of current (6-s long) indicated by the horizontal bars labeled "6 s" in panel A are superimposed and displayed on an expanded timescale. The vertical arrow indicates the initiation of the solution exchange. The smooth lines are the fitted curves for current development (n = 6). (C) Preexposing the cell to 10 mM Ba^{2+}, Mn^{2+}, or Mg^{2+} partially potentiated Ca^{2+}-I$_{CRAC}$, whereas Ni^{2+} and Zn^{2+} did not. (D) The time course of Ca^{2+}-I$_{CRAC}$ development when the cell was preexposed to 10 mM Ba^{2+} (taken from panel C), is shown on an expanded timescale. (E) The time course of Ca^{2+}-I$_{CRAC}$ development when the cell was preexposed to 10 mM Ni^{2+} (taken from panel C), is shown on an expanded timescale.

constant $\tau = 3.4 \pm 0.27$ s, $n = 6$; 15.0 ± 3.2 s; $n = 6$; and 4.2 ± 0.4 s, $n = 6$, respectively. These are slower than when the cell was preexposed to Ca^{2+}, but significantly faster than those when the cell was preexposed to Ni^{2+} ($P < 0.001$) and Zn^{2+} ($P < 0.001$). This is consistent with the finding that Ni^{2+} and Zn^{2+} could not potentiate Na^{+}-I$_{CRAC}$ in RBL cells (Fig. 3) but Ba^{2+}, Mn^{2+}, and Mg^{2+} were partially effective. The rapid increase in Ca^{2+}-I$_{CRAC}$ due to increased extracellular Ca^{2+} level when the potentiation site is fully occupied by Ca^{2+} suggests that Ca^{2+} binding to this site is necessary for the normal functioning of CRAC channels, as previously suggested for the CRAC channels in Jurkat T cells (Zweifach and Lewis, 1996; Christian et al., 1996), though slight differences clearly exist between these two cell types.

Ca^{2+} binding to the potentiation site is voltage dependent

We next tested the effect of transmembrane potential on Ca^{2+}-dependent potentiation of CRAC channels by mea-

suring the current evoked by applying an 80-ms voltage step of -80 mV from a holding potential (V_p) of 60, 0, or -60 mV at a frequency of 2 Hz. Fig. 7 A shows one of such experiments (the current displayed was taken at 70 ms after the initiation of the -80-mV voltage steps). As shown in Fig. 7, B–D, when the cell was exposed to SES, the increases in Ca^{2+}-I$_{CRAC}$ evoked by the -80-mV voltage steps from the indicated holding potential could be fitted to a single-exponential equation. However, the time constants of the current increase for preholding potentials -60 and 0 are significantly faster (0.203 ± 0.013 ms, $n = 10$ for -60 mV; 0.263 ± 0.009 ms, $n = 12$ for 0 mV) than for a preholding potential of 60 mV (0.738 ± 0.035 ms, $n = 14$, $P < 0.001$). These results suggest that positive transmembrane potential do not facilitate Ca^{2+}-I$_{CRAC}$. In addition, as shown in Fig. 7, A, E, and F, under the preholding potential of 60 mV, Ca^{2+} only slightly potentiated Na^{+}-I$_{CRAC}$, as its inactivation index (1.4 ± 0.1, $n = 5$) as well as its peak value (8.2 ± 1.2 pA/pF, $n = 5$) was significantly smaller than the respective values for preholding potentials of 0 (2.3 ± 0.2; 10.6 ± 0.7 pA/pF,
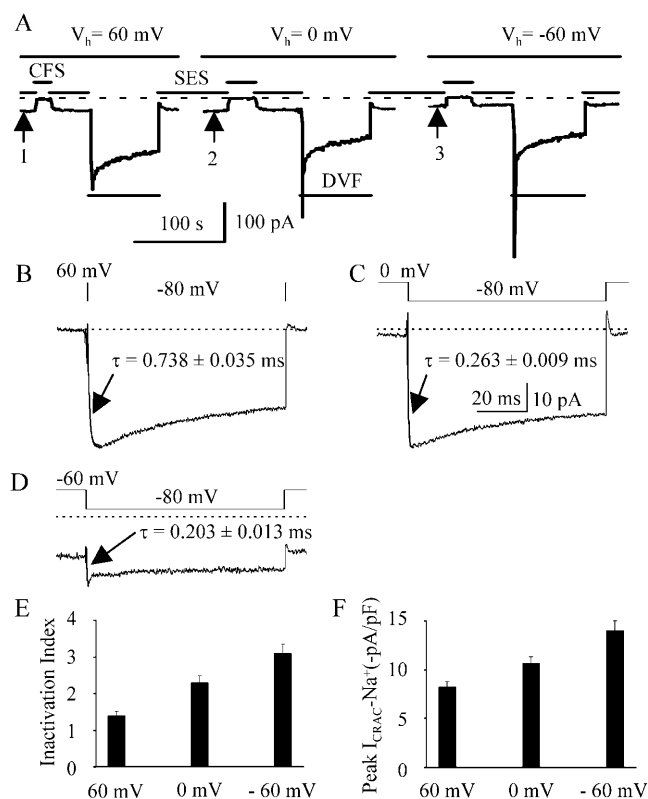
FIGURE 7 Ca^{2+} binding to the potentiation site is voltage dependent. (A) Currents were detected by 80-ms voltage steps of -80 mV from a holding potential (V_p) of 60, 0, or -60 mV. The current values at 70 ms after the initiation of the -80 mV voltage steps are displayed. The V_p values labeled above the horizontal bars indicate the holding potential between the -80 mV voltage steps. (B, C, and D) The averaged currents invoked by the indicated voltage steps, taken around the points labeled by arrows 1 ($n = 14$), 2 ($n = 12$), and 3 ($n = 10$) in panel A, respectively. (E) Inactivation index of Na^+-I_{CRAC} when $V_p = 60$, 0, or -60 mV, $n = 5$ for all cases. (F) The peak Na^+-I_{CRAC} when $V_p = 60$, 0, or -60 mV, $n = 5$ for all cases.

$n = 5$) and -60 mV (3.1 ± 0.3; 14.1 ± 1.0 pA/pF, $n = 5$). Data shown in Fig. 7, E and F, are pooled from experiments with different orders of voltage application to minimize the influence of the slow inactivation of I_{CRAC}. These results suggest that at positive transmembrane potentials, the binding affinity of Ca^{2+} to the potentiation site is lower, and hence, little potentiation of I_{CRAC} is seen. This result is consistent with the previous findings in Jurkat T cells by Zweifach and co-workers (Zweifach and Lewis, 1996).

DISCUSSION

The rapid inactivation of monovalent current through the CRAC channel is one of its striking characteristics, which might be used to identify this important yet elusive channel. In this study we have provided strong evidence that the inactivation of the Na^+-I_{CRAC} involves a Ca^{2+}-binding site on the channel, which we termed a Ca^{2+}-dependent potentiation site with a K_d of 186 nM. Ca^{2+} binding to this

site is required for the full functioning of CRAC channels as evidenced by the finding that Ca^{2+} occupation of this site accelerates the response to a change of extracellular Ca^{2+} level (Fig. 6). In other words, Ca^{2+} binding to this site potentiates the CRAC channels as suggested previously for Jurkat T cells (Zweifach and Lewis, 1996; Christian et al., 1996). Ba^{2+}, Mn^{2+}, and Mg^{2+} can also slightly potentiate the channel presumably by binding to the same site. That Mn^{2+} and Mg^{2+} can potentiate the CRAC channel suggests that the potentiation site is not located inside of the conducting pore, because CRAC channels do not permeate Mn^{2+} and Mg^{2+} (Figs. 1 A, 3 A, 6 C; also Hoth and Penner (1993) and Prakriya and Lewis (2002)). The potentiation site is likely located outside or at the outer mouth of the pore as suggested before for Jurkat T cells (Zweifach and Lewis, 1996; Christian et al., 1996).

Several results presented here strongly support the idea that Ca^{2+} ions dissociate from the permeation sites (e.g., Ca^{2+} sites in the selectivity filter) well before they dissociate from the potentiation sites when the extracellular solution is rapidly exchanged from Ca^{2+}-containing ones to DVF. First, the average K_d for the inhibition site (13.7 µM) is 74-fold higher than that for the potentiation site (186 nM). Second, when the Ca^{2+} level was not high enough (<100 µM) to completely block the CRAC channels, increase in $[Ca^{2+}]$ delayed the inactivation of Na^+-I_{CRAC} (Fig. 5, A and C), suggesting that the potentiation sites can be occupied by Ca^{2+} ions whereas the inhibition sites are not. And third, CRAC channels lose their selectivity well before undergoing a full inactivation (Fig. 1, C and D) during solution switch, suggesting that the relief of the inhibition of Na^+-I_{CRAC} by Ca^{2+} happens well before the loss of potentiation of Na^+-I_{CRAC} by Ca^{2+}.

In fact, modulation of ion channels by extracellular Ca^{2+} is not unique to the CRAC channel. It has been reported that Ca^{2+} potentiates nicotinic acetylcholine receptors (nAChRs) by binding to a site on the extracellular domain of the α-subunit of the nAChRs (Galzi et al., 1996; Le et al., 2002). Such binding greatly increases the open probability of nAChR channels and thus enhances the ensemble current, even if the unitary conductance decreases slightly (Mulle et al., 1992; Vernino et al., 1992). Armstrong and colleagues (Armstrong, 1999; Armstrong and Cota, 1991, 1999; Horn, 1999) have also demonstrated that Ca^{2+} occupancy of a site on the voltage-gated Na^+ channels in squid giant axon is required for channel closing and that nonoccupied channels fold reversibly into a nonfunctional conformation. Ca^{2+} occupancy of the potentiation site of CRAC channels also seems to be required for the channels to remain in a functional conformation, and nonoccupied channels appear to fold into a less functional conformation, because without Ca^{2+} binding to this site the channels are not fully permeable to Ca^{2+} even though they are in the fully active state (Fig.6, A and B). In other words, without Ca^{2+} occupancy at the potentiation site, only a small fraction of CRAC channels are

permeable to either Ca^{2+} or Na$^+$, and/or CRAC channels have a decreased single-channel conductance or open probability. However, the extremely small single-channel conductance of CRAC channels (Zweifach and Lewis, 1993; Prakriya and Lewis, 2002) prevents a detailed experimental analysis to provide further clarity.

Although CRAC channels in Jurkat T cells and RBL cells have many similar biophysical properties including inwardly rectifying I-V relationships, high Ca^{2+} selectivity, fast and slow inactivations, and rapid inactivation of monovalent cation currents (Zweifach and Lewis, 1995a,b; Parekh, 1998; Fierro and Parekh, 1999), they differ in some other properties. These include pore size, permeability to other cations in the absence of Ca^{2+} (Bakowski and Parekh, 2002), and responses to blockers (Su et al., 2002), suggesting that the molecular identities of CRAC channels in these two cell types are different. In this study, we found that the CRAC channel blockers Zn^{2+} and Ni^{2+} failed to potentiate I$_{CRAC}$ in RBL-2H3 cells when either Ca^{2+} or Na$^+$ were the permeating ions. This result is in contrast to findings with CRAC channels in Jurkat T cells, in which CRAC channels can be potentiated by Ni^{2+} as effectively as by Ca^{2+}. This provides additional evidence to support the idea that CRAC channels in Jurkat T and RBL cells are distinct subtypes within a CRAC channel family. Currently, there is intensive interest in the molecular cloning of CRAC channels (Clapham, 1996, 2002). This analysis may need to keep in mind the possibility of several subtypes of CRAC channels in different cell types or organisms.

The potentiation of CRAC channels by Ca^{2+} as well as the complex three-phase kinetics of I$_{CRAC}$ during the solution exchange can be easily explained considering the roles of the potentiation as well as the permeation sites on CRAC channels and their different affinities for Ca^{2+} (Fig. 8). Under normal physiological conditions, both types of the Ca^{2+} sites are occupied by Ca^{2+} ions. The Ca^{2+} occupancy of the permeation site, presumably located in or near the selectivity filter as suggested for voltage-gated Ca^{2+} channel

(Yang et al., 1993a; Ellinor et al., 1995a), prevents Na$^+$ from entering the pore even though [Na$^+$] is ~80 times higher than [Ca^{2+}] in the extracellular space. Ca^{2+} binding to the potentiation site insures the normal functioning of the channels (higher open probability or larger single-channel conductance). In the preactivation phase (phase I) of the Na$^+$-I$_{CRAC}$, the transient decrease in the current when the Ca^{2+}-containing solution is switched to the DVF, results from the anomalous mole fraction phenomena due to the decreased driving force of the Ca^{2+} current, and the concomitant blockage of the Na$^+$ current by Ca^{2+} binding to the permeation site. In the activation phase (phase II) when the [Ca^{2+}] further decreases, Ca^{2+} falls off the permeation site due to its lower affinity whereas the potentiation site is still occupied by Ca^{2+} because of its higher affinity, thus a robust Na$^+$ influx occurs, resulting in a larger current due at least to a larger unitary conductance for Na$^+$ (Prakriya and Lewis, 2002). As time elapses, Ca^{2+} begins to dissociate from the potentiation site because [Ca^{2+}] decreases further, resulting in the inactivation of current due to decreased open probability or single-channel conductance. Na$^+$-I$_{CRAC}$ thus enters the inactivation phase (phase III).

In summary, we have characterized a high-affinity Ca^{2+}-binding site on the outside of CRAC channels in RBL-2H3 cells. Ca^{2+} occupancy on this site potentiates I$_{CRAC}$ and such a potentiation is required for the normal functioning of CRAC channels. This signature property might be used to identify the molecular identity of CRAC channels.
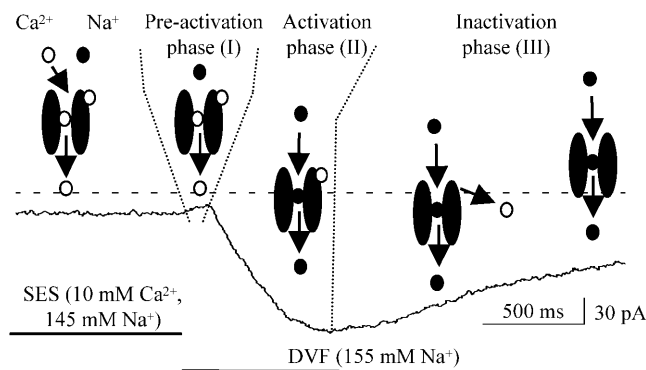
FIGURE 8 The working model to account for the three-phase kinetics of I$_{CRAC}$ when the extracellular solution is switched from the SES to the DVF (see text).

REFERENCES

Almers, W., and E. W. McCleskey. 1984. Non-selective conductance in calcium channels of frog muscle: calcium selectivity in a single-file pore. *J. Physiol.* 353:585–608.

Almers, W., E. W. McCleskey, and P. T. Palade. 1984. A non-selective cation conductance in frog muscle membrane blocked by micromolar external calcium ions. *J. Physiol.* 353:565–583.

Armstrong, C. M. 1999. Distinguishing surface effects of calcium ion from pore-occupancy effects in Na$^+$ channels. *Proc. Natl. Acad. Sci. USA.* 96:4158–4163.

Armstrong, C. M., and G. Cota. 1991. Calcium ion as a cofactor in Na$^+$ channel gating. *Proc. Natl. Acad. Sci. USA.* 88:6528–6531.

Armstrong, C. M., and G. Cota. 1999. Calcium block of Na+ channels and its effect on closing rate. *Proc. Natl. Acad. Sci. USA.* 96:4154–4157.

Bakowski, D., and A. B. Parekh. 2002. Monovalent cation permeability and Ca^{2+} block of the store-operated Ca^{2+} current I$_{CRAC}$ in rat basophilic leukemia cells. *Pflugers Arch.* 443:892–902.

Christian, E. P., K. T. Spence, J. A. Togo, P. G. Dargis, and J. Patel. 1996. Calcium-dependent enhancement of depletion-activated calcium current in Jurkat T lymphocytes. *J. Membr. Biol.* 150:63–71.

Clapham, D. E. 1996. TRP is cracked but is CRAC TRP? *Neuron.* 16:1069–1072.

Clapham, D. E. 2002. Sorting out MIC, TRP, and CRAC ion channels. *J. Gen. Physiol.* 120:217–220.

Ellinor, P. T., J. Yang, W. A. Sather, J. F. Zhang, and R. W. Tsien. 1995a. Ca^{2+} channel selectivity at a single locus for high-affinity Ca^{2+} interactions. *Neuron.* 15:1121–1132.

Ellinor, P. T., J. Yang, W. A. Sather, J. F. Zhang, and R. W. Tsien. 1995b. Ca^{2+} channel selectivity at a single locus for high-affinity Ca^{2+} interactions. *Neuron.* 15:1121–1132.

Fierro, L., and A. B. Parekh. 1999. Fast calcium-dependent inactivation of calcium release-activated calcium current (CRAC) in RBL-1 cells. *J. Membr. Biol.* 168:9–17.

Fukushima, Y., and S. Hagiwara. 1985. Currents carried by monovalent cations through calcium channels in mouse neoplastic B lymphocytes. *J. Physiol.* 358:255–284.

Galzi, J. L., S. Bertrand, P. J. Corringer, J. P. Changeux, and D. Bertrand. 1996. Identification of calcium binding sites that regulate potentiation of a neuronal nicotinic acetylcholine receptor. *EMBO J.* 15:5824–5832.

Hermosura, M. C., M. K. Monteilh-Zoller, A. M. Scharenberg, R. Penner, and A. Fleig. 2002. Dissociation of the store-operated calcium current I(CRAC) and the Mg-nucleotide-regulated metal ion current MagNuM. *J. Physiol.* 539:445–458.

Hess, P., J. B. Lansman, and R. W. Tsien. 1986. Calcium channel selectivity for divalent and monovalent cations. Voltage and concentration dependence of single channel current in ventricular heart cells. *J. Gen. Physiol.* 88:293–319.

Hess, P., and R. W. Tsien. 1984. Mechanism of ion permeation through calcium channels. *Nature.* 309:453–456.

Horn, R. 1999. The dual role of calcium: pore blocker and modulator of gating. *Proc. Natl. Acad. Sci. USA.* 96:3331–3332.

Hoth, M., and R. Penner. 1992. Depletion of intracellular calcium stores activates a calcium current in mast cells. *Nature.* 355:353–356 [see comments].

Hoth, M., and R. Penner. 1993. Calcium release-activated calcium current in rat mast cells. *J. Physiol. (Lond.).* 465:359–386.

Kozak, J. A., H. H. Kerschbaum, and M. D. Cahalan. 2002. Distinct Properties of CRAC and MIC Channels in RBL Cells. *J. Gen. Physiol.* 120:221–235.

Le, N. N., T. Grutter, and J. P. Changeux. 2002. Models of the extracellular domain of the nicotinic receptors and of agonist- and Ca^{2+}-binding sites. *Proc. Natl. Acad. Sci. USA.* 99:3210–3215.

Lewis, R. S., and M. D. Cahalan. 1989. Mitogen-induced oscillations of cytosolic Ca^{2+} and transmembrane Ca^{2+} current in human leukemic T cells. *Cell Regul.* 1:99–112.

Mulle, C., C. Lena, and J. P. Changeux. 1992. Potentiation of nicotinic receptor response by external calcium in rat central neurons. *Neuron.* 8:937–945.

Parekh, A. B. 1998. Slow feedback inhibition of calcium release-activated calcium current by calcium entry. *J. Biol. Chem.* 273:14925–14932.

Parekh, A. B., and R. Penner. 1997. Store depletion and calcium influx. *Physiol. Rev.* 77:901–930.

Prakriya, M., and R. S. Lewis. 2002. Separation and characterization of currents through store-operated CRAC channels and Mg^{2+}-inhibited cation (MIC) channels. *J. Gen. Physiol.* 119:487–507.

Premack, B. A., T. V. McDonald, and P. Gardner. 1994. Activation of Ca^{2+} current in Jurkat T cells following the depletion of Ca^{2+} stores by microsomal Ca^{2+}-ATPase inhibitors. *J. Immunol.* 152:5226–5240.

Putney, J. W. J., and G. S. Bird. 1993. The signal for capacitative calcium entry. *Cell.* 75:199–201.

Su, Z., D. S. Barker, P. Csutora, T. Chang, R. L. Shoemaker, R. B. Marchase, and J. E. Blalock. 2002. Regulation of Ca^{2+} release activated Ca^{2+} channels by INAD and calcium influx factor. *Am. J. Physiol. Cell Physiol.* 284:C497–C505.

Vernino, S., M. Amador, C. W. Luetje, J. Patrick, and J. A. Dani. 1992. Calcium modulation and high calcium permeability of neuronal nicotinic acetylcholine receptors. *Neuron.* 8:127–134.

Yang, J., P. T. Ellinor, W. A. Sather, J. F. Zhang, and R. W. Tsien. 1993a. Molecular determinants of Ca^{2+} selectivity and ion permeation in L-type Ca^{2+} channels. *Nature.* 366:158–161.

Yang, J., P. T. Ellinor, W. A. Sather, J. F. Zhang, and R. W. Tsien. 1993b. Molecular determinants of Ca^{2+} selectivity and ion permeation in L-type Ca^{2+} channels. *Nature.* 366:158–161.

Zweifach, A., and R. S. Lewis. 1993. Mitogen-regulated Ca^{2+} current of T lymphocytes is activated by depletion of intracellular Ca^{2+} stores. *Proc. Natl. Acad. Sci. USA.* 90:6295–6299.

Zweifach, A., and R. S. Lewis. 1995a. Rapid inactivation of depletion-activated calcium current (ICRAC) due to local calcium feedback. *J. Gen. Physiol.* 105:209–226.

Zweifach, A., and R. S. Lewis. 1995b. Slow calcium-dependent inactivation of depletion-activated calcium current. Store-dependent and -independent mechanisms. *J. Biol. Chem.* 270:14445–14451.

Zweifach, A., and R. S. Lewis. 1996. Calcium-dependent potentiation of store-operated calcium channels in T lymphocytes. *J. Gen. Physiol.* 107:597–610.